

Fig. 1S. The IR spectrum of $[4\text{-NH}_2\text{-2-Me(Q)H}][\text{VO}(\text{bcma})(\text{H}_2\text{O})]\text{2H}_2\text{O}$.

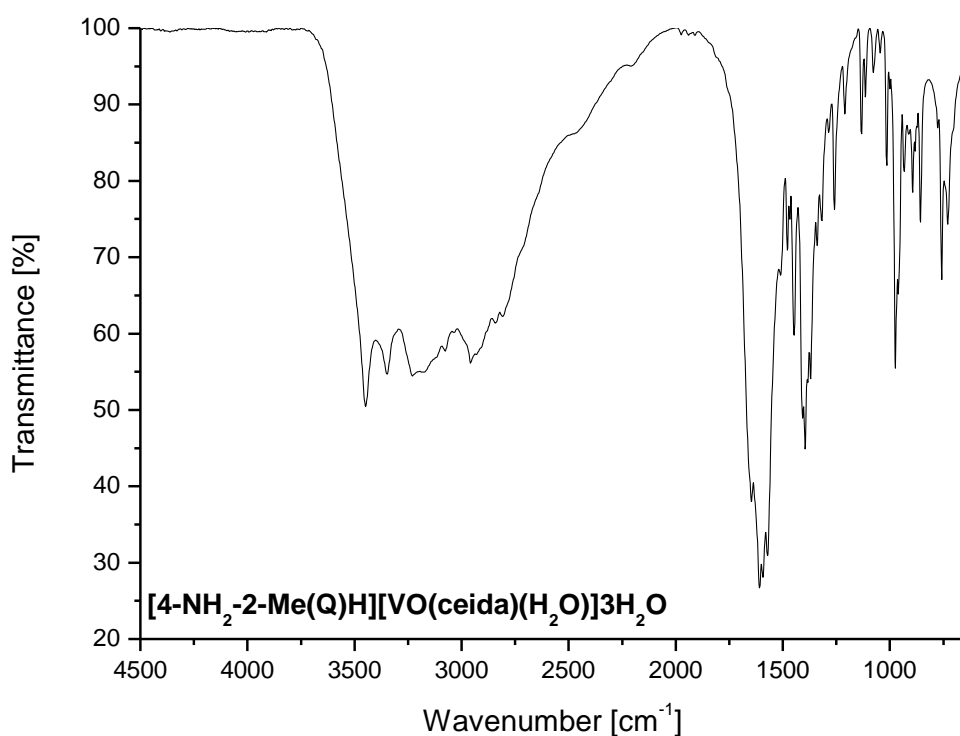


Fig. 2S. The IR spectrum of $[4\text{-NH}_2\text{-2-Me(Q)H}][\text{VO}(\text{ceida})(\text{H}_2\text{O})]\text{3H}_2\text{O}$.

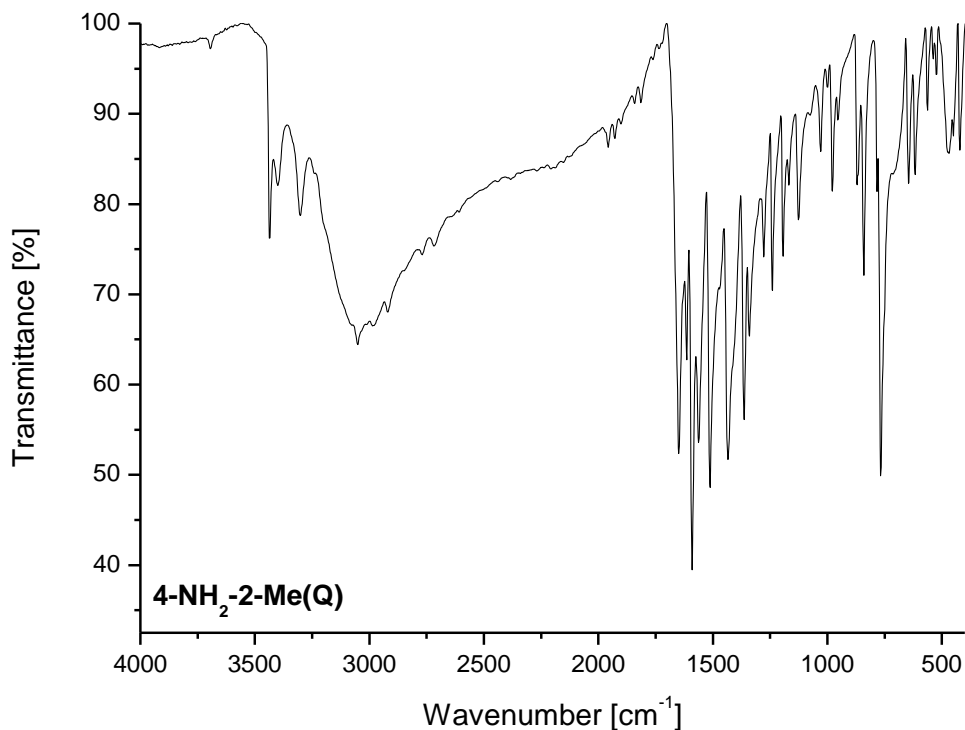


Fig. 3S. The IR spectrum of 4-NH₂-2-Me(Q).

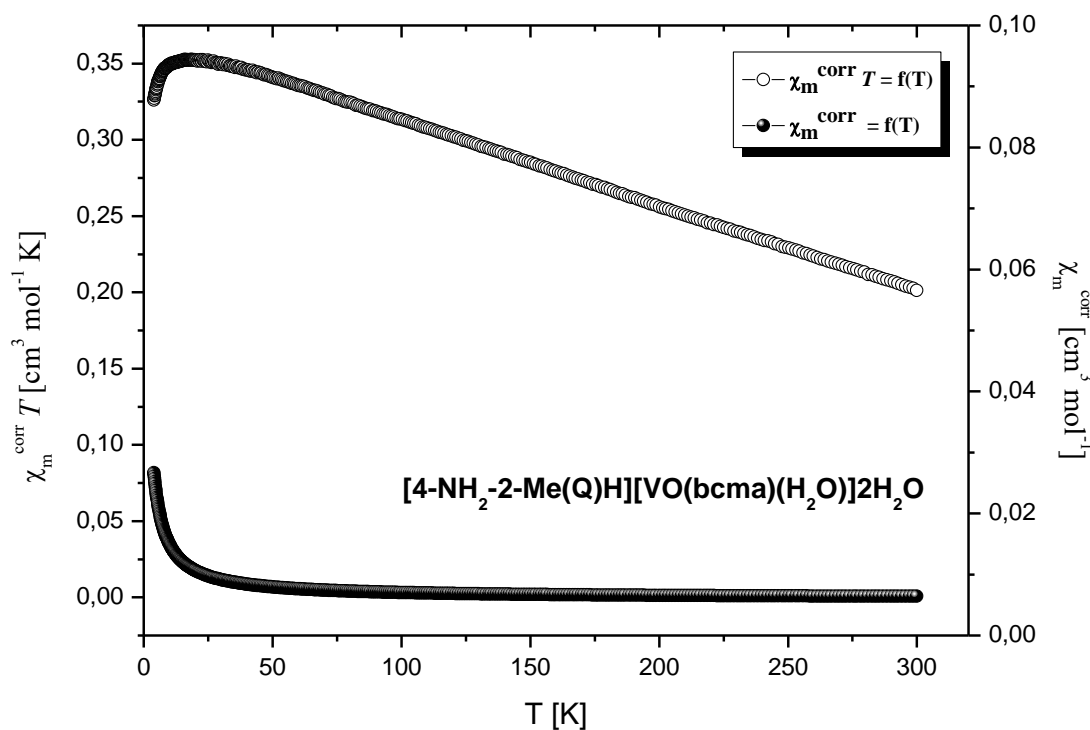


Fig. 4S. The temperature dependence of experimental $\chi_m T$ and χ_m (χ_m per one V(IV) ion) for [4-NH₂-2-Me(Q)H][VO(bcma)(H₂O)]²H₂O.

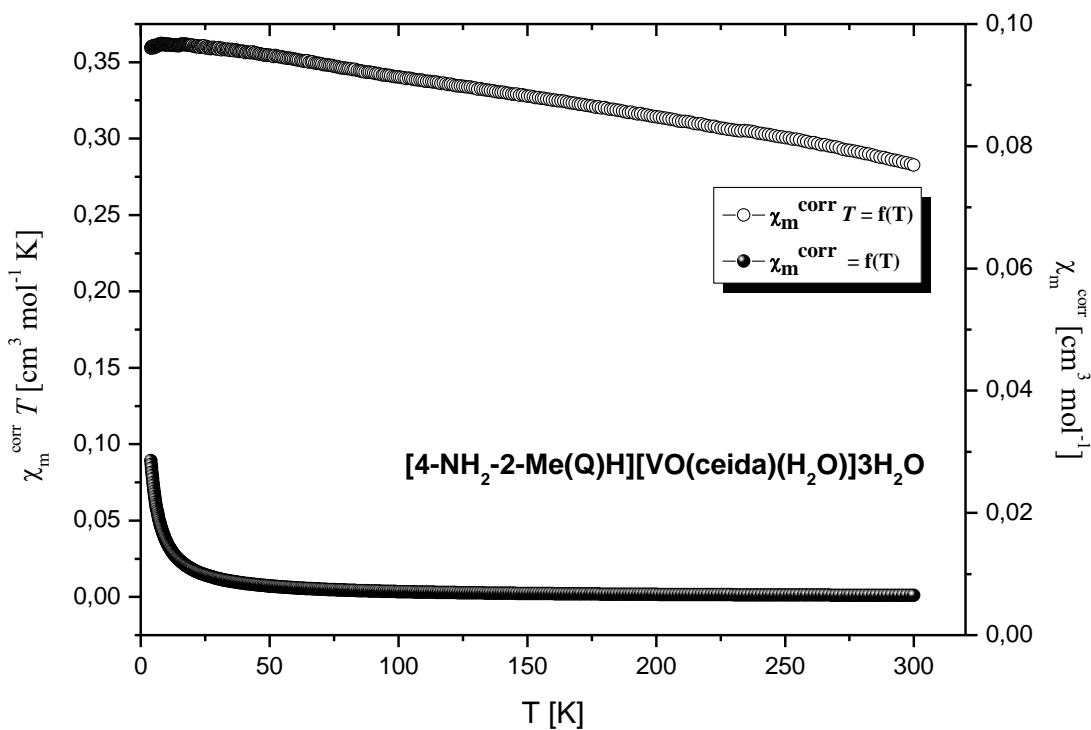


Fig. 5S. The temperature dependence of experimental $\chi_m T$ and χ_m (χ_m per one V(IV) ion) for $[4\text{-NH}_2\text{-2-Me(Q)H}][\text{VO(ceida)}(\text{H}_2\text{O})]\text{3H}_2\text{O}$.

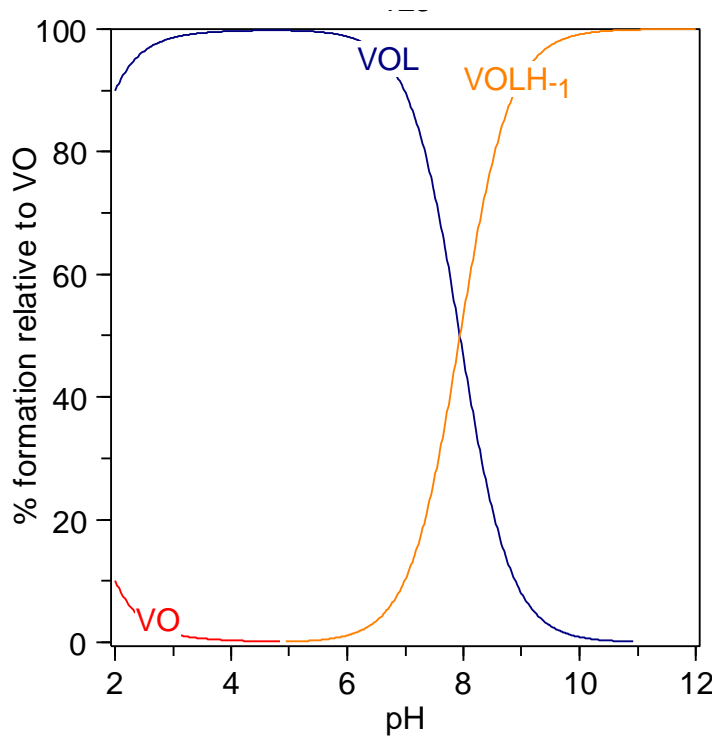


Fig. 6S. Concentration distribution curves of the species presented in the $[4\text{-NH}_2\text{-2-Me(Q)H}][\text{VO(bcma)}(\text{H}_2\text{O})]\text{2H}_2\text{O}$ solution as a function of the pH calculated based on the stability constants listed in Table 1.

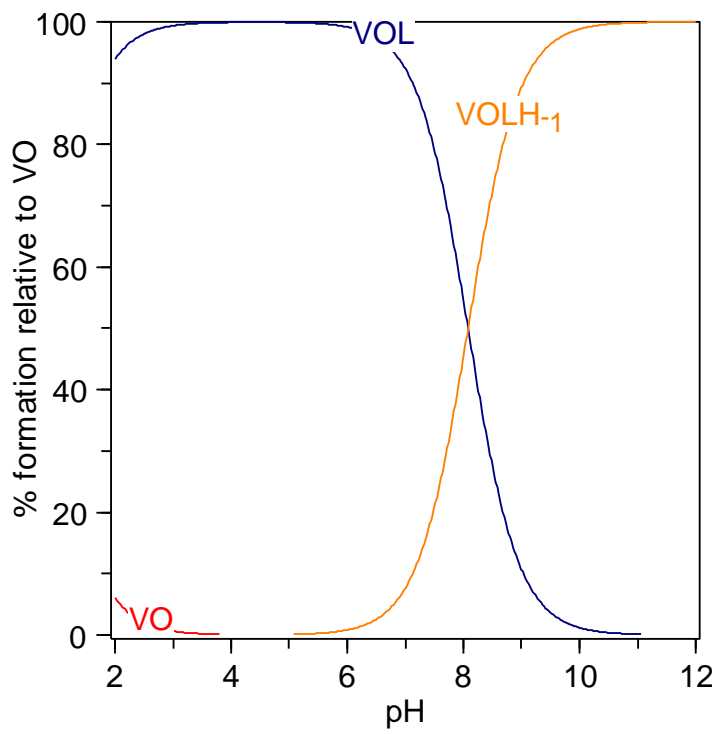


Fig. 7S. Concentration distribution curves of the species presented in the $[4\text{-NH}_2\text{-2-Me(Q)H}]_2[\text{VO(pmida)}]3\text{H}_2\text{O}$ solution as a function of the pH calculated based on the stability constants listed in Table 1.

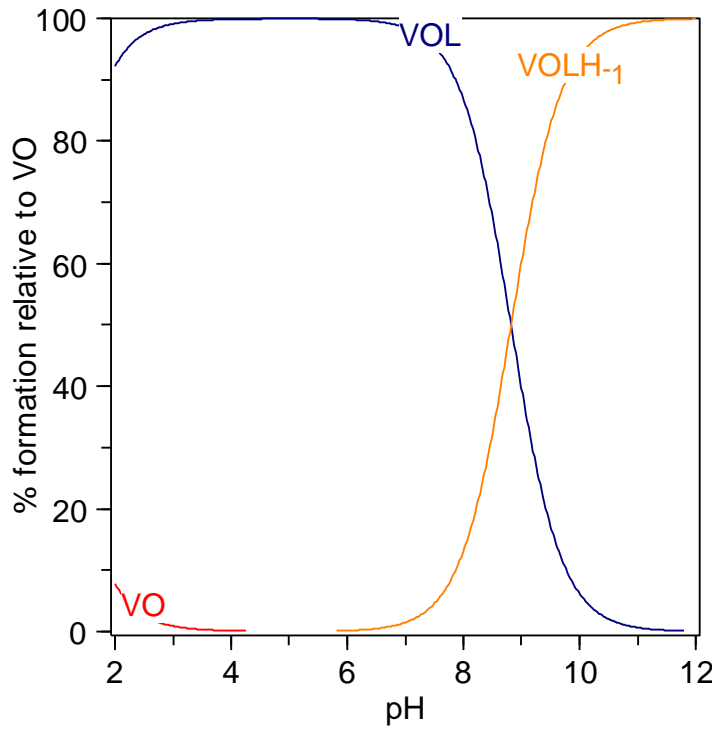


Fig. 8S. Concentration distribution curves of the species presented in the $[4\text{-NH}_2\text{-2-Me(Q)H}][\text{VO(ceida)}(\text{H}_2\text{O})]3\text{H}_2\text{O}$ solution as a function of the pH calculated based on the stability constants listed in Table 1.